Wormhole for electron waves in graphene

David E. Fernandes,[1] Nader Engheta,[2] and Mário G. Silveirinha[1],[*]

[1]*University of Coimbra, Department of Electrical Engineering–Instituto de Telecomunicações, 3030-290 Coimbra, Portugal*

[2]*University of Pennsylvania, Department of Electrical and Systems Engineering, Philadelphia, Pennsylvania 19104-6314, USA*

The theory of transformation optics for light has fascinated the scientific community for almost one decade due to its revolutionary and groundbreaking implications. Because the propagation of electrons in condensed-matter systems is also described by a wave equation, one may also envision the extension of this idea to matter waves. Here, we suggest that graphene can be used as a platform to demonstrate a "tunnel" or "wormhole" for electrons. Based on an effective medium approach, we theoretically demonstrate that two properly designed graphene-based nanomaterials can effectively "annihilate" one another from an electronic point of view, and provide for the delocalization of the wave-function stationary states, similar to a wormhole.

Graphene is a two-dimensional material characterized by a remarkably high crystal quality, and its unusual electronic "relativistic" spectrum creates many intriguing and exciting opportunities in low-dimensional physics, enabling one to mimic quantum relativistic phenomena in a condensed-matter system [1–7]. Low-energy electronics in graphene are governed by the massless Dirac equation. It has been shown that it is possible to gain some control over the propagation of charge carriers in graphene by applying a periodic electrostatic potential on graphene's surface. This can be done, for example, with periodically patterned gates, by deposition of adatoms, or by exploiting the potential induced by a crystalline substrate (e.g., boron nitride) [8–13]. These *graphene superlattices* (GSLs) have the potential to tailor the transport properties of electrons [14–16] and can lead to new inroads into nanoelectronics. Notably, in a recent series of works [17,18], we suggested that it may be possible to have an electron "perfect lens" in graphene based on the superlattice concept. This idea is the electronic counterpart of a perfect lens originally proposed in the context of electromagnetic metamaterials [19]. We demonstrated that in some conditions two materials with complementary properties may effectively behave as some form of "matter-antimatter" and annihilate one another from the electronic point of view, such that the paired materials provide a perfect "tunnel" for *any* extended or bounded stationary states. This is analogous to a "wormhole" that connects two regions of space, as if the region in between was nonexistent. Building on these studies, here we theoretically investigate the realization of electron wormholes based on one-dimensional (1D) graphene superlattices, and unveil the actual physical response provided by such structures. We envision this study may provide fertile ground for new physics in graphene electronics. Previous works have discussed the realization of light wormholes [20] based on transformation optics [21]. Moreover, other authors suggested electronic analogs of the Veselago-Pendry lens [22,23], and most remarkably, Ref. [22] showed that a *p-n* junction in graphene may mimic Veselago's lens under a semiclassical approximation. However, this is quite different from our proposal [17,18], which provides a

perfect electron "tunnel" even for bounded states and incoming waves with wide incidence angles. It is relevant to highlight that Klein tunneling ensures the complete transmission of an electron wave for normal incidence. However, for incident angles deviating from the normal direction an electron wave is typically strongly scattered by a single potential barrier [3–5]. Our results extend in a nontrivial manner Klein tunneling to electron waves with wide incident angles, including grazing incidence and evanescent waves.

We are interested in 1D graphene superlattices, such that the microscopic electrostatic potential has a step-type spatial variation [Fig. 1(a)], with two different values $V = V_{av} \pm V_{osc}$. It is well known that such 1D periodic potentials may yield strongly anisotropic Dirac cones and particle velocities, and may allow for the propagation of electron beams with virtually no diffraction [9,10]. Recently, we have proven that the low-energy states in GSLs can be characterized by an effective Hamiltonian that describes the dynamics of the wave-function envelope. For states with a pseudomomentum near the Dirac K point [3], the effective Hamiltonian may be taken equal to $(\hat{H}_{ef}\boldsymbol{\psi})(\mathbf{r}) = [-i\hbar v_F \boldsymbol{\sigma}(\chi) \cdot \nabla + V_{av}] \cdot \boldsymbol{\psi}(\mathbf{r})$, where $v_F \approx 10^6$ m/s is the Fermi velocity, $\boldsymbol{\sigma}(\chi) = \sigma_x \hat{\mathbf{x}} + \chi \sigma_y \hat{\mathbf{y}}$, σ_x, σ_y are the Pauli matrices, V_{av} is the average electrostatic potential in the superlattice [Fig. 1(a)], and χ is an effective medium parameter that we designate by *anisotropy ratio* and which depends on the fluctuating part V_{osc} of the microscopic potential [17]. Effective medium techniques have also been used to study the properties of excitons in semiconductor superlattices treated as anisotropic media [24,25]. As elaborated in the Supplemental Material [26], here we have slightly modified the formalism of Ref. [17] so that $\boldsymbol{\psi}^* \cdot \boldsymbol{\psi}$ can be regarded as a probability density function, and the time evolution of the pseudospinor $\boldsymbol{\psi}$ is determined by $i\hbar \partial_t \boldsymbol{\psi} = \hat{H}_{ef} \boldsymbol{\psi}$. Within this framework, the GSL may be regarded as a continuous medium. In particular, the stationary states energy dispersion is $|E - V_{av}| = \hbar v_F \sqrt{k_x^2 + \chi^2 k_y^2}$, which corresponds to a stretched Dirac cone [17]. The pseudospinor associated with a stationary state with energy E and wave vector $\mathbf{k} = (k_x, k_y)$ is of the form $\boldsymbol{\psi}_{E,k_y} = e^{i\mathbf{k}\cdot\mathbf{r}}(1 \quad se^{i\theta_q})^T/\sqrt{2}$. The parameter θ_q is equal to the angle between $\mathbf{q} = (k_x, \chi k_y)$ and the x axis and $s = \text{sgn}(E - V_{av})$, so that it is possible to write $se^{i\theta_q} = \hbar v_F (k_x + i \chi k_y)/(E - V_{av})$ [17].

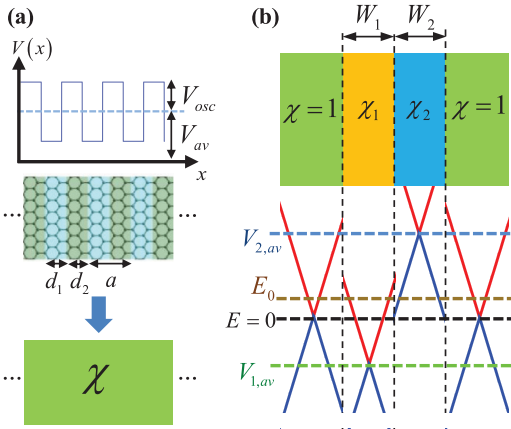[*]Author to whom correspondence should be addressed: mario.silveirinha@co.it.pt

FIG. 1. (Color online) (a) Sketch of a graphene superlattice characterized by a steplike periodic electrostatic potential $V(x) = V_{av} + V_{osc} \, \mathrm{sgn}[\sin(2\pi x/a)]$. (b) Geometry of two dual graphene superlattice slabs encapsulated in pristine graphene and the energy diagram associated with each material.

It was predicted in Refs. [17,18] that two GSLs with symmetric anisotropy ratios $\chi_1 = -\chi_2$ and equal x widths $W_1 = W_2$ are dual in the sense that for the energy level $E_0 = (V_{1,av} + V_{2,av})/2$ the superlattices have no effect on the wave propagation [Fig. 1(b)], so that any incoming electronic wave packet is tunneled through the paired GSLs as if they were absent. To demonstrate this idea, we designed two dual superlattices with $\chi_1 = -1/5.6$ and $\chi_2 = -\chi_1$ and a lattice period $a = 10$ nm. Using the theory of Ref. [17] it can be checked that these anisotropy ratios correspond to microscopic potentials with $V_{1,\mathrm{osc}} a/\hbar v_F \approx 7.83$ and $V_{2,\mathrm{osc}} a/\hbar v_F \approx 5.30$ [$V_{1,\mathrm{osc}} \approx 0.52$ eV and $V_{2,\mathrm{osc}} \approx 0.35$ eV]. It is supposed that the two superlattices have finite widths $W_1 = W_2 = 20a$ and are encapsulated in pristine graphene [Fig. 1(b)]. The energy scale is fixed so that $E = 0$ corresponds to the tip of the Dirac cone in pristine graphene (region $x < 0$). In the first example, the energy level wherein the perfect transmission is supposed to occur is set to $E_0 a/\hbar v_F = 0.3$. The average potentials in the superlattices are taken equal to $(V_{1,av} - E_0)a/\hbar v_F = -0.5$ and $(V_{2,av} - E_0)a/\hbar v_F = 0.5$. We use the transfer matrix formalism to characterize the scattering of an incoming electron plane wave ψ_{E,k_y}, propagating in pristine graphene with energy E and transverse quasimomentum k_y [16]. Assuming that the spatial variation along the y direction is of the form $e^{i k_y y}$, the transfer matrix $\mathbf{M} = \mathbf{M}(x, E, k_y, \chi)$ relates the wave function calculated at two points of space as $\psi(x_0 + x) = \mathbf{M} \cdot \psi(x_0)$. For a homogeneous region characterized by the parameters χ and V, the transfer matrix satisfies

$$\mathbf{M} = \begin{pmatrix} \cos(k_x x) + \chi k_y \frac{\sin(k_x x)}{k_x} & i\sqrt{k_x^2 + \chi^2 k_y^2} \frac{\sin(k_x x)}{s k_x} \\ i\sqrt{k_x^2 + \chi^2 k_y^2} \frac{\sin(k_x x)}{s k_x} & \cos(k_x x) - \chi k_y \frac{\sin(k_x x)}{k_x} \end{pmatrix},$$
(1)

where $s = \mathrm{sgn}\,(E - V)$ and k_x is the solution of $|E - V| = \hbar v_F \sqrt{k_x^2 + \chi^2 k_y^2}$. The above formula generalizes the theory of [16] to materials with nontrivial anisotropy ratio ($\chi \neq 1$). This will be useful later. Returning to the case of pristine graphene ($\chi = 1$), it is seen that because the pseudospinor is continuous

across the interfaces, the global transfer matrix for a cascade of $l = 1, \ldots, N$ homogeneous regions (with $V = V_l$ in the lth region) is $\mathbf{M}_{\mathrm{glob}} = \prod_{l=1}^{N} \mathbf{M}_l(d_l)$, where d_l is the thickness of the lth slab. Using this approach it is possible to compute the global transfer matrix that relates the wave function at the input and output interfaces, $\psi_o = \mathbf{M}_{\mathrm{glob}} \cdot \psi_i$, of the two dual graphene superlattices with total thickness $W_1 + W_2 = 40a$ ($N = 80$). Finally, the transmission (T) and reflection (R) coefficients can be found by solving the linear system:

$$\mathbf{M}_{\mathrm{glob}} \cdot \psi^+ + R\mathbf{M}_{\mathrm{glob}} \cdot \psi^- = T\psi^+, \qquad (2)$$

where $\psi^{\pm} = [1 \quad s_i(\pm k_{x,i} + i k_y)/\sqrt{k_{x,i}^2 + k_y^2}]^T$, and $k_{x,i}$ is the x-propagation constant of the incident wave. The calculated R and T for $E = E_0$ are depicted in Figs. 2(a) and 2(b) (discrete symbols) as a function of k_y. As seen, for incident waves with $|k_y| < k_{y,\mathrm{max}}$ with $k_{y,\mathrm{max}} a \approx 1.1$ the transmission coefficient satisfies to an excellent approximation $T \approx 1$, i.e., the amplitude is near unity and the phase is close to zero degrees. Hence, the paired GSLs indeed bridge the input and output interfaces of the structure behaving as a wormhole tunnel for electron waves. The parameter $k_{y,\mathrm{max}}$ may be regarded as the breaking point in the validity of the effective medium model. Note that that spectral region $|k_y| < k_{y,\mathrm{max}}$ includes all the propagating states in graphene at $E = E_0$. Indeed, it can be checked that $k_y = 0$ corresponds to normal incidence, whereas $k_y = k_{y0} \equiv E_0/\hbar v_F$ corresponds to grazing incidence. In the present example, $k_{y0} a = 0.3$ and thus $k_{y,\mathrm{max}} \approx 3.67 k_{y0}$. For $|k_y| > k_{y0}$ the incident electronic state is an evanescent wave, and cannot be normalized [17]. The performance of the paired GSLs is less satisfactory from the reflection point of view, because R is near zero only for $|k_y| < 0.4/a$.

The response of the paired superlattices can also be determined with the effective medium approach. Again, this can be done with the help of transfer matrices, but now there are two macroscopic regions and therefore we only need to consider two matrices ($N = 2$), which are calculated using Eq. (1) with $\chi = \chi_l$ and $V = V_{l,av}$ ($l = 1,2$). For $E = E_0$ this gives $T = 1$ and $R = 0$ for all k_y (a perfect "tunnel"), consistent with Refs. [17,18]. This macroscopic theory is based on the assumption that the macroscopic (envelope) pseudospinor is continuous at the interfaces of the different effective media, similar to the microscopic formulation. However, our numerical studies indicate that this hypothesis may lead to unsatisfactory results, as further discussed ahead. In truth, there is no compelling physical reason to enforce that the wave function is continuous in the macroscopic approach. The crucial requirement is that the *probability current density* j_x is continuous at the interfaces normal to the x direction. As shown in the Supplemental Material [26], in our case $j_x = v_F \psi^* \cdot \sigma_x \cdot \psi$. The continuity of j_x is evidently guaranteed by the continuity of ψ. However, this is not the only possibility. In fact, it can be checked that a generalized boundary condition of the type $\mathbf{U}_{x_0^-} \cdot \psi(x_0^-) = \mathbf{U}_{x_0^+} \cdot \psi(x_0^+)$ is compatible with the continuity of j_x at an interface $x = x_0$, with $\mathbf{U}_{x_0^{\pm}}$ linear operators that depend on the effective media, provided the $\mathbf{U}$ operators are such that $\mathbf{U}^{-1,\dagger} \cdot \sigma_x \cdot \mathbf{U}^{-1}$ is the same for all media. Because for pristine graphene $\mathbf{U}$ must be taken equal to the identity, it is necessary that $\mathbf{U}^{-1,\dagger} \cdot \sigma_x \cdot \mathbf{U}^{-1} = \sigma_x$. This
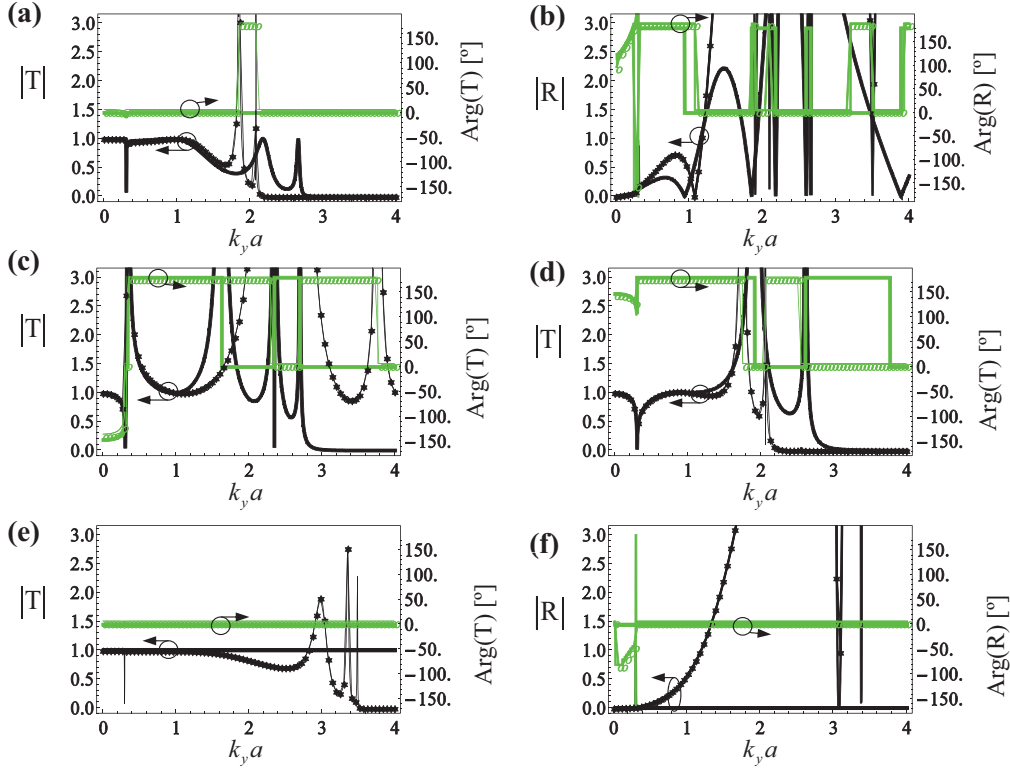
FIG. 2. (Color online) (a), (b) Amplitude and phase of the transmission and reflection coefficients for an electron plane wave that travels in pristine graphene with energy $E_0 a/\hbar v_F = 0.3$ and impinges on a slab of two dual GSLs with total thickness $W = 40a$, with $\chi_{1,2} = \mp 1/5.6$ and an average potential offset $(V_{1,2,av} - E_0) a/\hbar v_F = \mp 0.5$. (c) (superlattice 1) and (d) (superlattice 2) Amplitude and phase of the transmission coefficient of the individual GSLs taken separately. (e)–(f) Similar to (a) and (b) but for two dual GSLs with $\chi_{1,2} = 0$, The discrete symbols (joined by thin lines) correspond to the results calculated using the microscopic model, whereas the solid thick curves correspond to the effective medium model results.

can be satisfied if **U** commutes with σ_x and is unitary. Any **U** of the form

$$\mathbf{U} = e^{iu\sigma_x} = \begin{pmatrix} \cos u & i\sin u \\ i\sin u & \cos u \end{pmatrix}, \tag{3}$$

with u real valued, satisfies these restrictions. The parameter u depends on the effective medium parameters (χ) and for pristine graphene should be taken equal to zero. A numerical fitting of the microscopic and macroscopic model results shows that $u(\chi) = c_1 \arccos[1 + c_2(\chi - 1)]$ may accurately model the wave scattering at the interfaces with $c_1 = 0.689$ and $c_2 = 1.650$ [26]. In summary, we propose a boundary condition of the type $\lfloor \mathbf{U}(\chi) \cdot \boldsymbol{\psi} \rfloor_{x=x_0} = 0$ at the interface $x = x_0$, with $\lfloor F \rfloor_{x=x_0} \equiv F_{x=x_0^+} - F_{x=x_0^-}$. Within this framework, the global transfer matrix is given by $\mathbf{M}_{\mathrm{glob}} = \prod_{l=1}^{N} \mathbf{U}_l \cdot \mathbf{M}_l(d_l) \cdot \mathbf{U}_l^{-1}$. The reflection and transmitted coefficients are still computed by solving the linear system (2). The results obtained with this approach are depicted in Figs. 2(a) and 2(b) (thick solid lines), revealing a quite good agreement between the microscopic and the effective medium models, especially for $|k_y| < k_{y,\max}$.

Crucially, the combined effect of the two superlattices is essential to short-circuit the input and output regions and have the graphene wormhole. This is demonstrated by Figs. 2(c) and 2(d), which represent the individual response of each GSL. In Figs. 2(e) and 2(f), we report another design for the two dual GSL slabs, now with $\chi_1 = -\chi_2 = 0$

(this corresponds to $V_{\mathrm{osc},1} = V_{\mathrm{osc},2} \approx 6.28\hbar v_F/a \approx 0.42$ eV) and average potential offsets $(V_{1,2,av} - E_0)a/\hbar v_F = \mp 0.5$. Interestingly, in this case the corrected effective medium model with the boundary condition $\lfloor \mathbf{U}(\chi) \cdot \boldsymbol{\psi} \rfloor_{x=x_0} = 0$ predicts that the paired superlattices perfectly mimic a wormhole, such that $T = 1$ and $R = 0$ for all the incoming waves with energy E_0. Indeed, it can be checked that under the corrected effective medium model framework the conditions for perfect transmission are met when $u(\chi_1) = u(\chi_2)$, which is exactly satisfied only when $\chi_1 = -\chi_2 = 0$. In the example of Figs. 2(e)
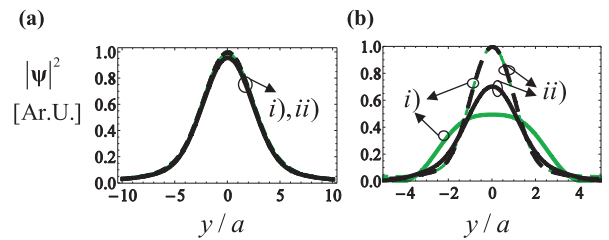

FIG. 3. (Color online) Profile of the wave-function amplitude $|\boldsymbol{\psi}|^2$ normalized to arbitrary unities (arb. units), at the input (dashed curves) and output (solid curves) interfaces of the graphene wormhole for an incoming packet with (a) $R_{G,1} = 2.86a$ and (b) $R_{G,2} = 1.14a$, calculated with (i) the microscopic model (green curves) and (ii) the effective medium model (black curves).

and 2(f), the microscopic and macroscopic theories agree up to $k_{y,\text{max}}a \approx 1.2$.

To illustrate how the dual GSLs may enable bridging the input and output regions for the case of an incoming spatially confined wave packet, we consider the scenario wherein a Gaussian electron wave impinges on the dual GSL nanomaterials. The Gaussian beam is taken equal to $\boldsymbol{\psi}^{\text{inc}}(x,y) = \int_{-\infty}^{+\infty} \boldsymbol{\psi}_{E_0,k_y}(x-x_i,y)e^{-k_y^2 R_G^2/4}dk_y$, where $\boldsymbol{\psi}_{E_0,k_y}$ is the pseudospinor for a plane wave stationary state with $E = E_0$ in pristine graphene. The parameter R_G can be regarded as the "beamwidth" at the reference plane $x_i = 0$, which is taken coincident with the input plane. We consider a dual GSL with the same parameters as in Figs. 2(a) and 2(b), except that the tunneling energy is set to $E_0 a/\hbar v_F = 0.025$ and the average potentials are adjusted to satisfy $(V_{1,2,\text{av}} - E_0)a/\hbar v_F = \mp 0.5$. For this design the conditions $T \approx 1$ and $R \approx 0$ are

approximately satisfied for $|k_y| < k_{y,\text{max}}$ with $k_{y,\text{max}}a \approx 1.1$. Hence, we can estimate that for a beam with a characteristic size larger than $R_{G,\text{min}} = \lambda_{\text{max}}/2 = 2.86a$ with $\lambda_{\text{max}} = 2\pi/k_{y,\text{max}}$ the dual GSL should mimic a wormhole at $E = E_0$. Figure 3 depicts the calculated wave-function profiles at the input and output planes for the cases (a) $R_{G,1} = R_{G,\text{min}}$ and (b) $R_{G,2} = R_{G,\text{min}}/2.5$. As seen, in case (a) the electron wave is perfectly reproduced at the output plane, whereas in case (b), when the localization is so fine that the response of spatial harmonics $|k_y| > k_{y,\text{max}}$ becomes relevant, the wave-function profiles at the input and output planes are quite different. Notably, in this example $R_{G,\text{min}}$ is extremely subwavelength as compared to the electron wavelength in pristine graphene at $E = E_0$ ($R_{G,\text{min}} = 0.011\lambda_0$). This elucidates how well the dual GSLs can effectively short-circuit the two interfaces and imitate a wormhole for electron waves.
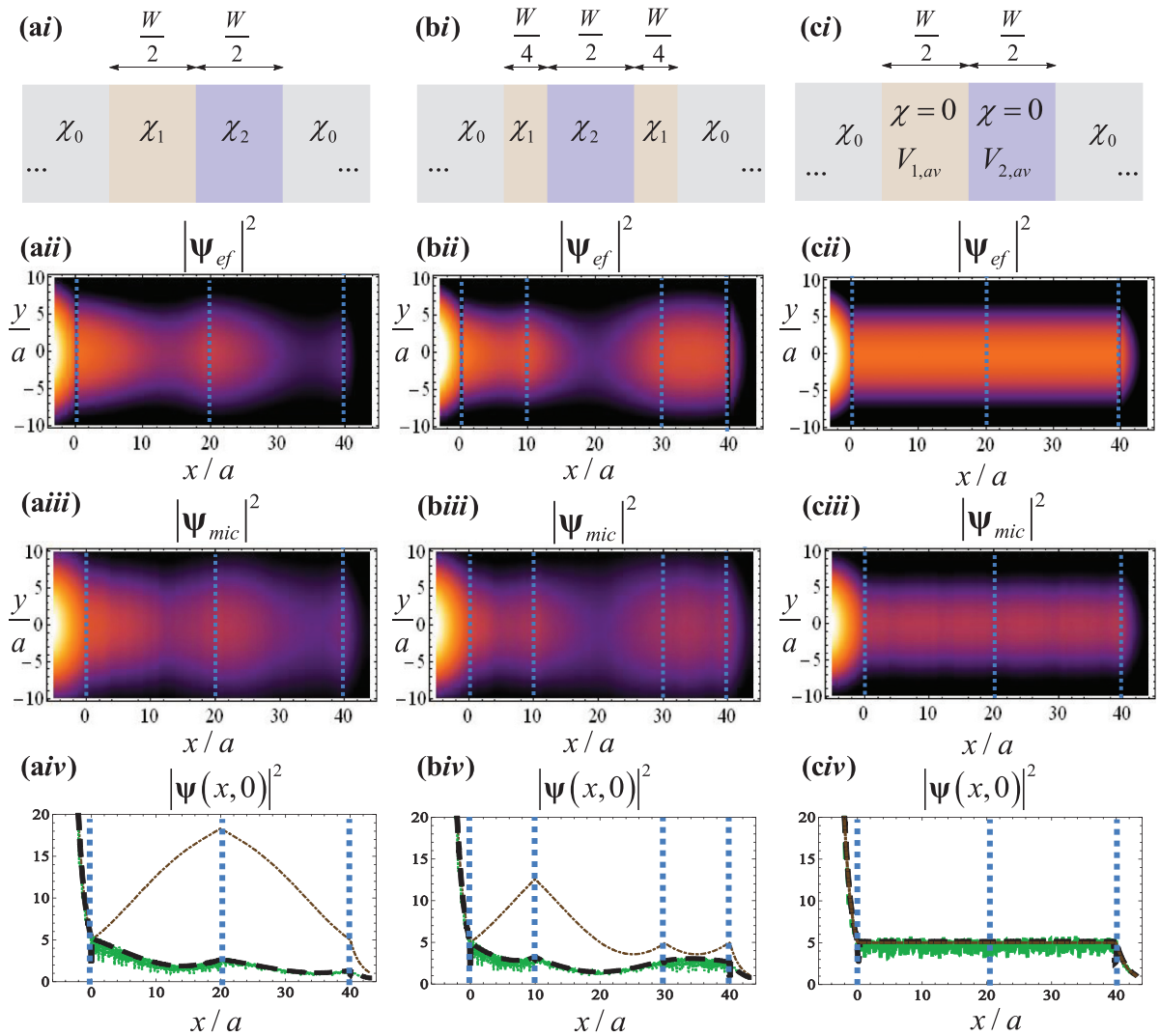

FIG. 4. (Color online) (i) Geometries of the different dual GSLs embedded in pristine graphene ($\chi_0 = 1$). (ii) Density plots of $|\boldsymbol{\psi}|^2$ (in a logarithmic scale) calculated with the effective medium theory for an incident Gaussian electron wave with $R_G = 2.86a$. (iii) Similar to (ii) but calculated with the exact microscopic theory. (iv) The pseudospinor profiles (normalized to arbitrary units, and along the $y = 0$ line) as a function of the x coordinate calculated using the microscopic model (green curves) and with the effective medium model (dashed thick black curves). The dot-dashed (brown) curves represent the results obtained with the effective medium model based on the simplistic boundary condition $\lfloor \boldsymbol{\psi} \rfloor_{x=x_0} = 0$. In all the examples, $E_0 a/\hbar v_F = 0.025$ and $(V_{1,2,\text{av}} - E_0)a/\hbar v_F = \mp 0.1$. In panels (a) and (b) the GSLs are such that $\chi_{1,2} = \mp 1/5.6$, whereas in panel (c) $\chi_{1,2} = 0$.

To further unravel the mechanisms that permit the nearly perfect transmission of the incoming electron wave, we computed the probability density distribution $|\psi|^2$ in all space using both the microscopic ($|\psi_{\mathrm{mic}}|^2$) and macroscopic ($|\psi_{\mathrm{ef}}|^2$) models. We consider two distinct configurations represented in Figs. 4(ai) and 4(bi). In both cases the total thickness of the two dual GSLs is the same. Thus, because dual GSLs with the same thickness "annihilate" one another, both configurations are expected to imitate a wormhole. In this example, we set $E_0 a/\hbar v_F = 0.025$, $(V_{1,2,\mathrm{av}} - E_0)a/\hbar v_F = \mp 0.1$, and the remaining structural parameters are as in Fig. 2(a). The Gaussian beam has a beamwidth $R_G = 2.86a$ at the reference plane $x_i = -5a$, and $x = 0$ is taken as the interface with the GSLs. The calculated distribution for $|\psi|^2$ is depicted in Figs. 4(a) and 4(b). As seen, there is good agreement between the effective medium model and the exact microscopic theory. Moreover, the results reveal that in this example the probability density function is peaked at the interfaces of the materials with symmetric χ. This should not be confused with the resonant behavior characteristic of Pendry's optical lens due to the excitation of plasmons [19], and of the HgCdTe semiconductor lens described in [18]. Indeed, it can be verified that most of the spatial spectrum inside the GSLs is associated with propagating waves. In panels (iv) of Fig. 4 we show $|\psi|^2$ calculated along the line $y = 0$. The dot-dashed lines in these plots represent the effective medium results based on the naive boundary condition $\lfloor\psi\rfloor_{x=x_0} = 0$. As seen, such approach highly overestimates the peak value of $|\psi|^2$, leading to a completely erroneous distribution for $|\psi|^2$. This reinforces the idea that in the effective medium framework the boundary condition is different from that of the microscopic theory.

As previously discussed, in the corrected effective medium theory the conditions $T = 1$ and $R = 0$ are exactly satisfied only when $\chi_1 = -\chi_2 = 0$. As seen in Fig. 4(c), for such a design, the electron wave is supercollimated along the direction of propagation with virtually no diffraction. This is consistent with the extreme anisotropy regime described in Refs. [9,10,17]. Moreover, in this example the wave-function profiles at the input and output planes are nearly coincident, further supporting that the dual GSLs mimic a wormhole. It is interesting to note that when $\chi = 0$ the transfer matrix **M** [Eq. (1)] is unitary and of the form $\mathbf{M} = \exp(\pm i \frac{|E-V_{\mathrm{av}}|}{\hbar v_F} x \sigma_x)$. Because this matrix is also independent of k_y it can be checked that in the effective medium framework $|\psi(x,y)|^2$ is independent of x in the GSL regions, consistent with Fig. 4(civ).

In summary, we theoretically demonstrated that dual GSLs may enable the perfect transmission of electron waves with a specific energy, and mimic a wormhole that effectively bridges the input and output interfaces. As a by-product, we found out that the dynamics of electron waves in graphene superlattices can be described using an effective medium approach based on a nontrivial boundary condition. The findings of this work, besides being of theoretical interest, may have far reaching implications in graphene electronics.

[1] K. S. Novoselov, A. K. Geim, S. V. Morozov, D. Jiang, M. I. Katsnelson, I. V. Grigorieva, S. V. Dubonos, and A. A. Firsov, Nature (London) **438**, 197 (2005).

[2] A. K. Geim and K. S. Novoselov, Nat. Mater. **6**, 183 (2007).

[3] A. H. Castro Neto, F. Guinea, N. M. R. Peres, K. S. Novoselov, and A. K. Geim, Rev. Mod. Phys. **81**, 109 (2009).

[4] M. I. Katsnelson, Mater. Today **10**, 20 (2007).

[5] M. I. Katsnelson, K. S. Novoselov, and A. K. Geim, Nat. Phys. **2**, 620 (2006).

[6] A. V. Rozhkov, G. Giavaras, Y. P. Bliokh, V. Freilikher, and F. Nori, Phys. Rep. **503**, 77 (2011).

[7] A. Vakil and N. Engheta, Science **332**, 1291 (2011).

[8] C. H. Park, L. Yang, Y. W. Son, M. L. Cohen, and S. G. Louie, Phys. Rev. Lett. **101**, 126804 (2008).

[9] C.-H. Park, L. Yang, Y.-W. Son, M. L. Cohen, and S. G. Louie, Nat. Phys. **4**, 213 (2008).

[10] C.-H. Park, Y.-W. Son, L. Yang, M. L. Cohen, and S. G. Louie, Nano Lett. **8**, 2920 (2008).

[11] J. C. Meyer, C. O. Girit, M. F. Crommie, and A. Zettl, Appl. Phys. Lett. **92**, 123110 (2008).

[12] M. Yankowitz, J. Xue, D. Cormode, J. D. Sanchez-Yamagishi, K. Watanabe, T. Taniguchi, P. Jarillo-Herrero, P. Jacquod, and B. J. LeRoy, Nat. Phys. **8**, 382 (2012).

[13] L. A. Ponomarenko, R. V. Gorbachev, G. L. Yu, D. C. Elias, R. Jalil, A. A. Patel, A. Mishchenko, A. S. Mayorov, C. R. Woods, J. R. Wallbank, M. Mucha-Kruczynski, B. A. Piot, M. Potemski, I. V. Grigorieva, K. S. Novoselov, F. Guinea, V. I. Fal'ko, and A. K. Geim, Nature (London) **497**, 594 (2013).

[14] Y. P. Bliokh, V. Freilikher, S. Savel'ev, and F. Nori, Phys. Rev. B **79**, 075123 (2009).

[15] P. Burset, A. L. Yeyati, L. Brey, and H. A. Fertig, Phys. Rev. B **83**, 195434 (2011).

[16] L.-G. Wang and S.-Y. Zhu, Phys. Rev. B **81**, 205444 (2010).

[17] M. G. Silveirinha and N. Engheta, Phys. Rev. B **85**, 195413 (2012).

[18] M. G. Silveirinha and N. Engheta, Phys. Rev. Lett. **110**, 213902 (2013).

[19] J. B. Pendry, Phys. Rev. Lett. **85**, 3966 (2000).

[20] A. Greenleaf, Y. Kurylev, M. Lassas, and G. Uhlmann, Phys. Rev. Lett. **99**, 183901 (2007).

[21] J. B. Pendry, D. Schurig, and D. R. Smith, Science **312**, 1780 (2006); U. Leonhardt, *ibid.* **312**, 1777 (2006); V. M. Shalaev, *ibid.* **322**, 384 (2008).

[22] V. V. Cheianov, V. Fal'ko, and B. L. Altshuler, Science **315**, 1252 (2007).

[23] I. Hrebikova, L. Jelinek, J. Voves, and J. D. Baena, Photonics Nanostruct.: Fundam. Appl. **12**, 9 (2014).

[24] M. F. Pereira, Jr., I. Galbraith, S. W. Koch, and G. Duggan, Phys. Rev. B **42**, 7084 (1990).

[25] M. F. Pereira, Jr., Phys. Rev. B **52**, 1978 (1995).

[26] See Supplemental Material at http://link.aps.org/supplemental/10.1103/PhysRevB.90.041406 for materials about the effective medium model.